Transportation Research Part B 57 (2013) 361–377

Contents lists available at SciVerse ScienceDirect

Transportation Research Part B

journal homepage: www.elsevier.com/locate/trb

A multi-commodity Lighthill–Whitham–Richards model of lane-changing traffic flow ☆

Wen-Long Jin *

Department of Civil and Environmental Engineering, California Institute for Telecommunications and Information Technology, Institute of Transportation Studies, University of California, 4000 Anteater Instruction and Research Bldg, Irvine, CA 92697-3600, United States

ARTICLE INFO

Keywords:
Macroscopic lane-changing behaviors
Multi-commodity Lighthill–Whitham–Richards model
Fundamental diagram
Entropy condition
Flux function
Demand

ABSTRACT

Systematic lane changes can seriously deteriorate traffic safety and efficiency inside lane-drop, merge, and other bottleneck areas. In our previous studies (Jin, 2010a,b), a phenomenological model of lane-changing traffic flow was proposed, calibrated, and analyzed based on a new concept of lane-changing intensity. In this study, we further consider weaving and non-weaving vehicles as two commodities and develop a multi-commodity, behavioral Lighthill–Whitham–Richards (LWR) model of lane-changing traffic flow. Based on a macroscopic model of lane-changing behaviors, we derive a fundamental diagram with parameters determined by car-following and lane-changing characteristics as well as road geometry and traffic composition. We further calibrate and validate fundamental diagrams corresponding to a triangular car-following fundamental diagram with NGSIM data. We introduce an entropy condition for the multi-commodity LWR model and solve the Riemann problem inside a homogeneous lane-changing area. From the Riemann solutions, we derive a flux function in terms of traffic demand and supply. Then we apply the model to study lane-changing traffic dynamics inside a lane-drop area and show that the smoothing effect of HOV lanes is consistent with observations in existing studies. The new theory of lane-changing traffic flow can be readily incorporated into Cell Transmission Model, and this study could lead to better strategies for mitigating bottleneck effects of lane-changing traffic flow.

© 2013 Elsevier Ltd. All rights reserved.

1. Introduction

In the seminal Lighthill–Whitham–Richards (LWR) model by (Lighthill and Whitham, 1955; Richards, 1956), traffic dynamics on a road link are described by the evolution of density $k(x, t)$, speed $v(x, t)$, and flow-rate $q(x, t)$ at location x and time t. Physically, the LWR model captures kinematic shock and rarefaction waves in traffic flow; mathematically, it is a scalar hyperbolic conservation law. The model can be defined by the following rules:

R1. The constitutional law of continuous media: $q = kv$.
R2. The fundamental diagram of a speed-density relation in steady states: $v = V(x, t, k)$,[1] from which we can have a flow-density relation: $q = Q(x, t, k) \equiv kV(x, t, k)$.

☆ This paper was presented at the 20th International Symposium on Transportation & Traffic Theory. It therefore also appears in the complete proceedings of the 20th ISTTT in [Procedia – Social and Behavioral Sciences, vol. 80C (2013), pp. aaa–bbb].

* Tel.: +1 949 824 1672.
E-mail address: wjin@uci.edu

[1] On a homogeneous road with identical vehicles, $v = V(k)$ is independent of both location and time.

0191-2615/$ - see front matter © 2013 Elsevier Ltd. All rights reserved.
http://dx.doi.org/10.1016/j.trb.2013.06.002

R3. Traffic conservation: $\frac{\partial k}{\partial t}+\frac{\partial q}{\partial x}=0$.
R4. Weak solutions: discontinuous shock waves can develop from continuous initial conditions (Smoller, 1983).
R5. Entropy conditions: physical weak solutions of the LWR model must satisfy some entropy conditions (Lax, 1972).

From the first three rules one can derive the following LWR model

$$\frac{\partial k}{\partial t}+\frac{\partial kV(x,t,k)}{\partial x}=0. \tag{1}$$

Since (1) is a hyperbolic conservation law, R4 and R5 have to be implicitly assumed in order to obtain unique, physical solutions. Among the aforementioned five rules, R1, R3, and R4 are self-evident and applies to many systems, but different types of traffic systems warrant their specific R2 and R5. Related to R2, there have been many studies on fundamental diagrams (e.g. Greenshields, 1935; Del Castillo and Benitez, 1995a,b): speed usually decreases in density, and flow-rate is unimodal in density. In contrast, R5 is highly related to drivers' dynamic car-following behaviors: in Ansorge (1990), it was shown that the traditional Lax entropy condition, which states that shock waves arise if and only if characteristic waves cross each other, for the LWR model on a homogeneous road is consistent with the observation that a shock wave forms when vehicles decelerate, and a rarefaction wave forms when vehicles accelerate. The LWR model can be directly applied for traffic on multi-lane roads, if vehicles on all lanes share the same characteristics; i.e., if a single-class traffic stream travels on a single-lane-group road.

It is well known that systematic lane changes on multi-lane roads can have significant impacts on overall traffic safety and characteristics (e.g. Golob et al., 2004; Cassidy and Rudjanakanoknad, 2005; Ahn and Cassidy, 2007; Patire and Cassidy, 2011). Many lane-changing models have been developed to determine vehicles' dynamic decisions on whether, why, when, where, and how a vehicle changes its lane at the microscopic level (Gipps, 1986; Yang, 1997; Hidas, 2002; Toledo et al., 2003; Kesting et al., 2007). In Laval and Daganzo (2006), a hybrid model of lane-changing traffic was proposed by considering lane-changing vehicles as moving bottlenecks with bounded acceleration rates, and it was shown that systematic lane changes could cause capacity drops. More follow-up studies along this line can be found in Laval et al. (2005) and Laval and Leclercq (2008). Impacts of lane changes on traffic characteristics have also been extensively studied at the macroscopic level: levels of service inside weaving areas measured by the speeds of weaving and non-weaving vehicles (e.g. Leisch, 1979), the distribution of weaving and non-weaving traffic on rightmost lanes (e.g. Cassidy et al., 1989), and dynamic capacities of a weaving section (Eads et al., 2000; Rakha and Zhang, 2006).

In Jin (2010a,b), a phenomenological lane-changing traffic flow model was proposed within the framework of the LWR theory by introducing a new fundamental diagram (R2) and a corresponding entropy condition (R5): first, the lane-changing intensity, $\epsilon(x,t)$, was defined as the ratio of the total lane-changing time over the total travel time in an Edie's spatial–temporal domain (Edie, 1963); second, a functional relation between ϵ and total density $k, \epsilon = E(x,k)$, was calibrated with the NGSIM data sets (Federal Highway Administration, 2006); third, based on the observation that a vehicle occupies two lanes during its lane-changing process, the speed-density relation derived from car-following behaviors was modified to include the effects of lane changes: $v = V(k\cdot(1+\epsilon))$; fourth, the LWR model of lane-changing traffic can be written as

$$\frac{\partial k}{\partial t}+\frac{\partial kV(k\cdot(1+E(x,k)))}{\partial x}=0; \tag{2}$$

finally, in a special case when ϵ is location-dependent, an inhomogeneous LWR model is derived and solved with an additional entropy condition proposed by (Isaacson and Temple, 1992).

The LWR model (2) provides a simple framework for studying lane-changing traffic dynamics, but is limited since the intensity-density relation is exogenous and has to be calibrated for different locations inside a lane-changing area. In addition, intuitively lane-changing traffic characteristics should be related to the composition of weaving and non-weaving vehicles.[2] For example, in a lane-changing area around an on-ramp, lane changes are primarily induced by vehicles from on-ramps, and freeway and on-ramp traffic streams can have different contributions to lane changes and therefore the total traffic dynamics. This observation inspires us to model lane-changing traffic within the framework of multi-commodity LWR models. In the new model, weaving and non-weaving vehicles are considered as two commodities. Then from a macroscopic model of lane changes, we derive a fundamental diagram, in which travel speed depends on densities of both commodities as well as car-following and lane-changing characteristics. The new fundamental diagram is calibrated and validated with NGSIM data. The resulting multi-commodity LWR model can be solved with corresponding entropy conditions. We apply the new theory to study lane-changing traffic around a lane-drop area and provide an explanation of observed smoothing effects of HOV lanes. Compared with the exogenous intensity-density relation in Jin (2010a,b), the intensity-density relation and, therefore, the fundamental diagram are endogenous and can be derived from traffic composition, road geometry, and lane-changing characteristics. In this sense, the new one is a behavioral lane-changing model.

The rest of the paper is organized as follows. In Section 2, we present a multi-commodity LWR model of lane-changing traffic flow. In Section 3, we derive a multi-commodity fundamental diagram. In Section 4, we present an example of lane-changing fundamental diagram and its calibration and validation. In Section 5, we solve the Riemann problem for

[2] Here by weaving vehicles we mean those that cannot continue on their current lanes, either because the lanes will merge or are not on their paths. Therefore, weaving vehicles may not be in a weaving area.

the multi-commodity LWR model. In Section 6, we develop a multi-commodity LWR model for the lane-changing area around a lane-drop bottleneck and study the smoothing effect of HOV lanes. In Section 7, we conclude the study with some future research directions.

2. A multi-commodity LWR model of lane-changing traffic flow

On a multiple-lane-group road, we separate a multi-class traffic stream into P commodities according to vehicles' attributes,[3] and the set of commodities is denoted by Ω. At (x, t), the density, speed, and flow-rate of commodity $\omega \in \Omega$ are denoted by $k_\omega(x, t)$, $v_\omega(x, t)$, and $q_\omega(x, t)$, respectively. Then we have vectors of densities, $\mathbf{k}(x, t)$, speeds, $\mathbf{v}(x, t)$, and flow-rates, $\mathbf{q}(x, t)$. Then the evolution of commodity traffic flows can be described by the multi-commodity LWR model.

2.1. Review of multi-commodity LWR models

Similar to the traditional LWR model, the multi-commodity LWR model can be defined by the following rules:

R1′. The constitutional law: $\mathbf{q} = \mathbf{k} \circ \mathbf{v}$, where $\circ$ is an entry-wise product.
R2′. The fundamental diagram: speed-density relations, $\mathbf{v} = \overrightarrow{V}(x, t, \mathbf{k})$, where $\overrightarrow{V}(x, t, \cdot)$ is a vector of size P; and flow-density relations, $\mathbf{q} = \overrightarrow{Q}(x, t, \mathbf{k}) \equiv \mathbf{k} \circ \overrightarrow{V}(x, t, \mathbf{k})$.
R3′. Traffic conservation: $\frac{\partial \mathbf{k}}{\partial t} + \frac{\partial \mathbf{q}}{\partial x} = 0$.
R4′. Weak solutions: discontinuous shock waves can develop from initially smooth data.
R5′. Entropy conditions: solutions should be unique and satisfy some physical laws.

Then from R1′, R2′, and R3′, the multi-commodity LWR model can be written as

$$\frac{\partial \mathbf{k}}{\partial t} + \frac{\partial \mathbf{k} \circ \overrightarrow{V}(x, t, \mathbf{k})}{\partial x} = 0, \tag{3}$$

which is a system of P hyperbolic conservation laws. Here the independent variables are P commodity densities. From R1′, the relation between total and commodity quantities are in the following ((x, t) omitted unless necessary):

$$k = \sum_{\omega \in \Omega} k_\omega, \quad q = \sum_{\omega \in \Omega} q_\omega,$$
$$v = \frac{q}{k} = \frac{\sum_{\omega \in \Omega} k_\omega v_\omega}{\sum_{\omega \in \Omega} k_\omega} = \frac{\sum_{\omega \in \Omega} q_\omega}{\sum_{\omega \in \Omega} q_\omega / v_\omega}.$$

Note that the LWR model for the total density, (1), can also be included in the model with $P - 1$ equations of commodity densities. Similar to the LWR model of single-commodity traffic flow, (1), the multi-commodity LWR model, (3), is well-defined for specific traffic flow systems, when fundamental diagram (R2') and entropy conditions (R5') are consistent with their static and dynamic characteristics.

In the literature, the multi-commodity LWR model was studied for partial flows in Lebacque (1996, Section 7). In the study all commodities observe the first-in-first-out (FIFO) principle and share the same speed at the same location and time, which is a function of total density; i.e., $v_\omega = V(x, t, k)$. In this case, the multi-commodity LWR model is consistent with the single-commodity LWR model and has been incorporated into a multi-commodity discrete kinematic wave model of network traffic (Jin and Zhang, 2004). In Jin (2012), a continuous kinematic wave theory was further developed for multi-commodity network traffic.

In Daganzo (1997), a multi-commodity LWR model was developed for traffic flow on a roadway with HOV lanes. A multi-commodity fundamental diagram was proposed for high-occupancy and low-occupancy vehicles, and the Riemann problem was discussed for one- and two-pipe regimes. A scheme was developed in Daganzo et al. (1997) to solve the problem numerically. Furthermore, a multi-commodity model was developed for slow and fast vehicles on general multi-lane roads in Daganzo (2002).

In Benzoni-Gavage and Colombo (2003), a multi-population LWR model similar to (3) was derived for heterogeneous drivers with a general R2', and commodity-dependent speed-density relations were used in simulations: $v_\omega = V_\omega(k)$.

In Wong and Wong (2002), a multi-class LWR model similar to (3) was derived for heterogeneous drivers with a general R2', but a homogeneous speed-density relation was used in simulations: $v_\omega = V(k)$, with which the model becomes essentially the same as that in Lebacque (1996).

In Zhang and Jin (2002), a multi-commodity LWR model was developed for mixed traffic, in which vehicles with different free-flow speeds have different contributions to the fundamental diagram: $v_\omega = V(\mathbf{k})$. Traditional entropy conditions were used to pick out unique, physical solutions for the Riemann problem, and it was shown that vehicles follow the FIFO principle in the model.

[3] Here vehicles' attributes are usually related to their travel characteristics, such as paths, classes (trucks, HOV), aggressiveness, etc. But non-travel attributes such as colors can also be used to determine commodities.

More studies on multi-commodity traffic flow models and their numerical solutions can be found in Chanut and Buisson (2003), Burger and Kozakevicius (2007), Bürger et al. (2008), van Lint et al. (2008), Ngoduy (2010) and references therein. To the best of our knowledge, however, no multi-commodity LWR models have been proposed for lane-changing traffic flow.

2.2. A macroscopic lane-changing model

Since weaving vehicles can induce disruptive lane changes and have contributions to traffic dynamics different from non-weaving vehicles, it is reasonable to consider weaving vehicles as one commodity, and non-weaving vehicles as another commodity. For total traffic, its density, speed, and flow-rate are denoted by k, v, and q, respectively[4]; for weaving traffic, its density, speed, and flow-rate are denoted by ρ, ψ, and ϕ, respectively. Then, for non-weaving traffic, its density, speed, and flow-rate are $k-\rho$, $(kv-\rho\psi)/(k-\rho)$, and $q-\phi$, respectively. We assume that the speed-density relations are location- and time-independent inside a lane-changing area; i.e., $v = V(k,\rho)$, and $\psi = \Psi(k,\rho)$, then we can obtain the following two-commodity LWR model of lane-changing traffic:

$$\frac{\partial k}{\partial t}+\frac{\partial kV(k,\rho)}{\partial x}=0, \tag{4a}$$

$$\frac{\partial \rho}{\partial t}+\frac{\partial \rho\Psi(k,\rho)}{\partial x}=0. \tag{4b}$$

Even though vehicles can overtake each other inside a lane-changing area, it was shown that in a congested area the difference in speeds for weaving and non-weaving vehicles is less than 5 mph (Roess et al., 1974). Therefore we can assume that traffic streams are balanced across all lanes on a congested road. That is, all lanes belong to the same lane-group. Therefore, for a multi-class, single-lane-group lane-changing traffic system, we have the following proposition.

Proposition 2.1. *Inside a lane-changing area, weaving and non-weaving vehicles have the same speed at the same location and time. That is, $V(k,\rho) = \Psi(k,\rho)$ in (4).*

From Proposition 2.1, we can replace $\Psi(k,\rho)$ by $V(k,\rho)$ in (4b) and simplify the multi-commodity LWR model (4) of lane-changing traffic flow as follows:

$$\frac{\partial k}{\partial t}+\frac{\partial kV(k,\rho)}{\partial x}=0, \tag{5a}$$

$$\frac{\partial \rho}{\partial t}+\frac{\partial \rho V(k,\rho)}{\partial x}=0. \tag{5b}$$

If we denote the proportion of weaving vehicles by

$$\xi=\rho/k, \tag{6}$$

then from (5) we have

$$\frac{\mathrm{d}\xi}{\mathrm{d}t}=\frac{\partial \xi}{\partial t}+V(k,\rho)\frac{\partial \xi}{\partial x}=0. \tag{7}$$

That is, the profile of ξ travels along vehicles, and the FIFO principle is observed in the lane-changing model (5).

Note that, however, (5) is incomplete. In order for the model to be well-defined, in the following sections we will propose a fundamental diagram (R2') and entropy conditions (R5'), which should be consistent with static and dynamic characteristics of lane-changing traffic flow.

3. A multi-commodity fundamental diagram of lane-changing traffic

Without loss of generality, we denote the upstream and downstream boundaries of an n-lane lane-changing area by 0 and L,[5] respectively. For lane-changing vehicles, their longitudinal trajectories in a space–time domain are illustrated in Fig. 1, in which the red line segments denote the trajectories when they are changing lanes. According to the definitions by (Edie, 1963), the average density in a space–time domain shown in Fig. 1 is vehicle-hours traveled divided by the domain's area. That is,

$$k=\frac{\sum_{j=1}^{J} t_j}{LT}, \tag{8}$$

where L is the length of the lane-changing area, T the time duration, J the number of vehicles inside the domain, and t_j the travel time of vehicle j.

[4] Hereafter we omit (x,t) for these quantities unless necessary.

[5] In reality the length of the lane-changing area may not be fixed under different traffic conditions.

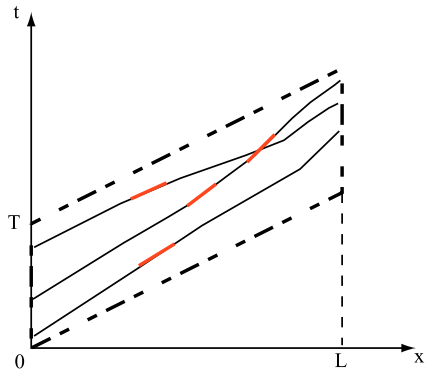

Fig. 1. Longitudinal trajectories of lane-changing vehicles inside a lane-changing area: x is the longitudinal coordinate.

3.1. Lane-changing intensity

In lane-changing areas, however, a vehicle occupies two lanes and equals two vehicles effectively during its lane-changing process, and the lane-changing duration of a lane-changing vehicle should be double counted in the total vehicle-lane-hours in order to obtain the effective average density on each lane. That is, the average density on each lane is $\bar{k}/n$, where the effective density $\bar{k}$ equals vehicle-lane-hours traveled divided by the space–time domain's area. Thus,

$$\bar{k} = \frac{\sum_{j=1}^{J} t_j + N_{LC}\pi}{LT}, \tag{9}$$

where N_{LC} is the number of lane changes and π the average lane-changing duration. As shown in Jin (2010b), the value of π depends on the definition of a lane change in the lateral movement.

Then the lane-changing intensity can be defined as (Jin, 2010a)

$$\epsilon = \frac{\bar{k}}{k} - 1 = \frac{N_{LC}\pi}{\sum_{j=1}^{J} t_j} = \frac{N_{LC}\pi}{kLT}. \tag{10}$$

In Jin (2010a,b), it was shown that $\epsilon(x, t)$ is well-defined as an aggregate variable just like density, speed, and flow-rate, and can be calculated from vehicle trajectory data in a spatio-temporal domain.

Inside a congested lane-changing area, we assume that all lanes are fully balanced. That is, densities and speeds are the same at the same location and time across different lanes. Therefore, the effective density on each lane becomes $z = \frac{\bar{k}}{n} = \frac{k(1+\epsilon)}{n}$. Note that, without considering lane changes, we have $z = \frac{k}{n}$, and the additional effective density can capture the bottleneck effect of lane changes. Furthermore, we assume that the speed-density relation is the same on all lanes and determined by car-following behaviors: $v = F(z)$, which usually satisfies the following properties: (i) Speed decreases in density; i.e., $\frac{dv}{dz} \leqslant 0$; (ii) $G(z) \equiv zF(z)$ is unimodal with a critical density z_c, capacity $z_cF(z_c)$, and critical speed $v_c = F(z_c)$; (iii) The free-flow speed $F(0) = v_f$ is finite; i.e., $G(0) = 0$; (iv) At the jam density z_j, $F(z_j) = 0$. Since $G(z)$ is unimodal, then $G'(z)(z - z_c) < 0$. Thus $V'(z) < 0$ when $z > z_c$; but $V'(z) \geqslant 0$ when $z < z_c$. One example is the triangular fundamental diagram (Munjal et al., 1971; Haberman, 1977; Newell, 1993):

$$F(z) = \min\left\{v_f, \frac{1}{\tau}\left(\frac{1}{z} - \frac{1}{z_j}\right)\right\}, \tag{11}$$

where τ is the time gap (Newell, 2002). Another example is the Greenshields fundamental diagram (Greenshields, 1935):

$$F(z) = v_f\left(1 - \frac{z}{z_j}\right).$$

Then incorporating the lane-changing intensity into the car-following speed-density relation, we can obtain the following speed-density relation in lane-changing traffic:

$$v = F\left(\frac{\bar{k}}{n}\right) = F\left(\frac{k(1+\epsilon)}{n}\right). \tag{12}$$

In Jin (2010a,b), exogenous relations between ϵ and k at different locations were calibrated such that $\epsilon = E(x, k)$. Then (12) becomes a location-dependent fundamental diagram, and (5) becomes a single-commodity model. In this study, in contrast, we attempt to derive an endogenous relation between ϵ and commodity traffic densities, k and ρ.

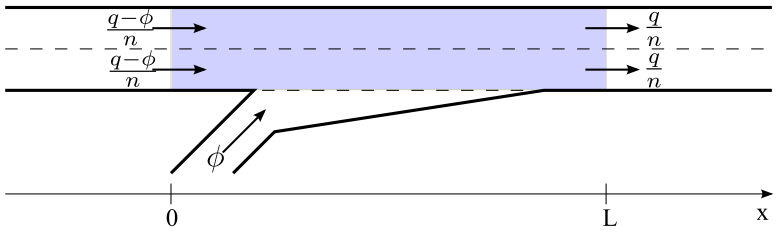

Fig. 2. The lane-changing area around an on-ramp.

3.2. A macroscopic lane-changing model

In this subsection, we develop a model of N_{LC} inside a lane-changing area downstream of a merge, as shown in Fig. 2.[6] In this lane-changing area, it is reasonable to assume that on-ramp vehicles are weaving vehicles, since they induce all lane changes.[7] In addition, we assume that traffic is steady and uniform inside the lane-changing area during [0, T]: all lanes have the same density, speed, and flow-rate, and the flow-rate of on-ramp vehicles inside the lane-changing area equals the on-ramp flow-rate, ϕ. At the upstream boundary of the lane-changing area, the flow-rate on each lane is $\frac{q-\phi}{n}$, and at the downstream boundary, the flow-rate on each lane becomes $\frac{q}{n}$. Since initially all on-ramp vehicles merge to the shoulder lane, $\frac{\phi T}{n}$ vehicles will switch to each lane inside the lane-changing area. Then the number of lane changes can be computed by

$$N_{LC} = \frac{\phi T}{n} \cdot (n-1) + \cdots + \frac{\phi T}{n} \cdot 1 = \frac{n-1}{2} \phi T. \tag{13}$$

From (13) we can see that: (i) the number of lane changes in a spatial–temporal domain is proportional to the number of vehicles that have to change lanes, ϕT, by assuming that traffic tends to be balanced in the lane-changing area; and (ii) the number of lane changes increases in the number of lanes, but the relationship depends on the geometry of the lane-changing area. Some additional remarks on (13) are in order: (i) This relationship is similar to Eq. (22) in Jin (2010a), but here ϕ is the flow-rate of on-ramp vehicles inside the lane-changing area, which is related to the on-ramp flow-rate but may not be the same in non-steady traffic; (ii) In reality, traffic is not steady, and the formula is meant to work for average traffic. That is, we expect scattered dots in the $N_{LC} - \phi$ plot in non-uniform traffic, as scattered dots in observed flow-density relations.

3.3. A lane-changing fundamental diagram

If we assume that the lane-changing duration π is constant,[8] we can have from (10) and (13)

$$\epsilon = \alpha \frac{\phi}{k}, \tag{14}$$

where $\alpha = \frac{n-1}{2L}\pi$. Here the parameter α is related to the road geometry parameter n, vehicles' lane-changing behavioral characteristics π, and the characteristics of lane-changing area L. Note that, if ϕ is constant, (14) is similar to one relation calibrated in Jin (2010a), but here the lane-changing intensity is also a function of the weaving flow-rate, ϕ.

Combining (12) and (14), we have the following multi-commodity speed-density relation in lane-changing traffic

$$v = F\left(\frac{k+\alpha\phi}{n}\right) = F\left(\frac{(1+\alpha\xi v)k}{n}\right), \tag{15a}$$

which leads to an implicit function of v in k and ξ

$$v = V(k, \xi). \tag{15b}$$

The corresponding flow-density relations are

$$q = kF\left(\frac{k+\alpha\phi}{n}\right), \tag{16a}$$

$$\rho = \frac{\phi}{F\left(\frac{k+\alpha\phi}{n}\right)}. \tag{16b}$$

[6] We assume that the lane-changing area includes a section upstream to the on-ramp, since non-weaving vehicles can switch to left lanes to avoid merging vehicles.

[7] Here we assume that this is an isolated on-ramp, so that lane changes induced by diverging vehicles can be ignored.

[8] In reality, the lane-changing duration differs for different vehicles and traffic conditions (Toledo and Zohar, 2007). Therefore, this is a first-order approximation of the lane-changing duration.

Then (15) and (16), (14), and (6) constitute the lane-changing fundamental diagram.

Different from the car-following fundamental diagram, in which the total density is the only independent variable, the lane-changing fundamental diagram has two independent variables out of the seven variables, k, ρ, ξ, ϵ, v, q, and ϕ:

- If k and ϕ are given, we can first calculate v from (15), then q and ρ from (16), ϵ from (14), and ξ from (6).
- If ρ and k are given, we can first calculate ξ from (6), then v from (15), $q = kv$ and $\phi = \rho v$, and ϵ from (14).
- If ρ and ξ are given, we can first solve v from (15), then $q = kv$ and $\phi = \rho v$, ρ from (6), and ϵ from (14).

Clearly the lane-changing fundamental diagram depends on the road geometry parameter, n, car-following characteristics including the free-flow speed, v_f, time-gap, τ, and jam density, z_j, and lane-changing characteristics including the lane-changing area length, L, and the lane-changing duration, π.

4. Calibration and validation of a lane-changing fundamental diagram

In this section, we propose a lane-changing fundamental diagram based on a triangular car-following fundamental diagram, (11), in which the critical density per lane is given by

$$z_c = \frac{z_j}{1 + \tau z_j v_f}. \tag{17}$$

The triangular fundamental diagram is consistent with General Motors and other car-following models as well as observations (Haberman, 1977; Newell, 2002). In this section, we first derive the fundamental diagram using different independent variables, then calibrate parameters related to road geometry, car-following, and lane-changing with NGSIM data for a lane-changing area on I-80, and finally validate the intensity-, speed-, and flow-rate-density relations with the same data sets.

4.1. Total density and weaving flow-rate as independent variables

When k and ϕ are known, ϵ can be directly computed from (14). Further from (15) and (16), we obtain the following lane-changing fundamental diagram:

$$v = V(k,\phi) \equiv \min\left\{v_f, \frac{1}{\tau}\left(\frac{n}{k+\alpha\phi} - \frac{1}{z_j}\right)\right\}, \tag{18a}$$

$$q = Q(k,\phi) \equiv \min\left\{v_f k, \frac{1}{\tau}\left(\frac{nk}{k+\alpha\phi} - \frac{k}{z_j}\right)\right\}, \tag{18b}$$

$$\rho = \phi / \min\left\{v_f, \frac{1}{\tau}\left(\frac{n}{k+\alpha\phi} - \frac{1}{z_j}\right)\right\}. \tag{18c}$$

Since $0 \leqslant v \leqslant v_f$ and $\phi \leqslant q$, the domains of k and ϕ are given by $\phi \geqslant 0$, $k \geqslant 0$, and

$$k + \alpha\phi \leqslant nz_j,$$
$$\phi \leqslant \min\left\{v_f k, \frac{1}{\tau}\left(\frac{nk}{k+\alpha\phi} - \frac{k}{z_j}\right)\right\}.$$

We denote $Q_2(k,\phi) = \frac{1}{\tau}\left(\frac{nk}{k+\alpha\phi} - \frac{k}{z_j}\right)$, which is defined for $nz_j - \alpha\phi \geqslant k \geqslant nz_c - \alpha\phi$. Then $\frac{\partial Q_2(k,\phi)}{\partial k} = \frac{n\alpha\phi}{(k+\alpha\phi)^2} - \frac{1}{z_j}$ decreases in k. Therefore $Q_2(k, \phi)$ is concave in k.

Then the capacity of a lane-changing area can be computed from the fundamental diagram in (18) as follows:

- When

$$\phi \leqslant \frac{nz_c^2}{\alpha z_j}, \tag{19}$$

$Q_2(k, \phi)$ decreases in k for $k \geqslant nz_c - \alpha\phi$. In this case, $Q(k, \phi)$ reaches its maximum when $k = nz_c - \alpha\phi$. Therefore, the capacity of the lane-changing area for a given ϕ is

$$Q^{max}(\phi) = v_f(nz_c - \alpha\phi).$$

Without lane changes, the capacity is $nz_c v_f$. Thus the capacity reduction caused by lane-changing traffic is

$$CR = \frac{nz_c v_f - Q^{max}(\phi)}{nz_c v_f} = \frac{\alpha\phi}{nz_c} \leqslant \frac{z_c}{z_j}.$$

- When $\phi > \frac{nz_c^2}{\alpha z_j}$, $Q_2(k,\phi)$ reaches its capacity at $k = \sqrt{nz_j\alpha\phi} - \alpha\phi$, and the capacity is

$$Q^{max}(\phi) = \frac{1}{\tau z_j}\left(\sqrt{nz_j} - \sqrt{\alpha\phi}\right)^2,$$

and the capacity reduction caused by lane-changing traffic is

$$CR = \frac{nz_c v_f - Q^{max}(\phi)}{nz_c v_f} > \frac{z_c}{z_j}.$$

4.2. Total density and weaving proportion as independent variables

When k and ξ are known, from (15) we have

$$v = \min\left\{v_f, \frac{1}{\tau}\left(\frac{n}{k(1+\alpha\xi v)} - \frac{1}{z_j}\right)\right\}.$$

When $v < v_f$, we have $v = \frac{1}{\tau}\left(\frac{n}{k(1+\alpha\xi v)} - \frac{1}{z_j}\right)$, which yields

$$k = K_2(v,\xi) \equiv \frac{nz_j}{(1+\alpha\xi v)(1+\tau z_j v)}. \tag{20a}$$

Hence, $K_2(0,\xi) = nz_j$, and $K_2(v_f,\xi) = nz_c/(1+\alpha\xi v_f)$. Since $\frac{\partial K_2(v,\xi)}{\partial v} < 0$, the inverse function of $k = K_2(v,\xi)$ exists and is denoted by $v = K_2^{-1}(k,\xi)$. Hence the speed-density relation can be written as

$$v = V(k,\xi) \equiv \min\left\{v_f, K_2^{-1}(k,\xi)\right\}. \tag{20b}$$

Then we have the following intensity function

$$\epsilon = E(k,\xi) = \alpha\xi v = \min\{\alpha v_f\xi, \alpha\xi K_2^{-1}(k,\xi)\}, \tag{20c}$$

and the corresponding flow-density relation:

$$q = Q(k,\xi) = \begin{cases} Q_1(k,\xi) \equiv v_f k, & k \leqslant nz_c/(1+\alpha\xi v_f) \\ Q_2(k,\xi) \equiv kK_2^{-1}(k,\xi), & k > nz_c/(1+\alpha\xi v_f) \end{cases} \tag{20d}$$

When $k > nz_c/(1+\alpha\xi v_f)$, or, equivalently, when $v < v_f$, q is also a function of v:

$$q = \widetilde{Q}_2(v,\xi) \equiv vK_2(v,\xi) = \frac{nv}{(1+\alpha\xi v)(1/z_j + \tau v)}, \quad \text{when } v < v_f \tag{20e}$$

Clearly, $\frac{\partial Q_2(k,\xi)}{\partial\xi} < 0$; i.e., the total flow-rate decreases in the proportion of weaving vehicles in congested traffic. In addition, $\frac{\partial\widetilde{Q}_2(v,\xi)}{\partial v} = \frac{n(1/z_j - \alpha\tau\xi v^2)}{(1+\alpha\xi v)^2(1/z_j+\tau v)^2}$ decreases in v. Therefore, $\widetilde{Q}_2(v,\xi)$ is concave in v.

Then the capacity of a lane-changing area can be computed from the fundamental diagram in (20) as follows:

- When $1/z_j - \alpha\tau\xi v_f^2 \geqslant 0$, or when

$$(n-1)\xi \leqslant \frac{2L}{\pi\tau z_j v_f^2},$$

$\widetilde{Q}_2(v,\xi)$ increases in v for $v \leqslant v_f$, and $Q_2(k,\xi)$ decreases in k. In this case, $Q(k,\xi)$ reaches its maximum when

$$z_c(\xi) = \frac{nz_c}{1+\alpha\xi v_f}, \tag{21a}$$

$$v_c(\xi) = v_f. \tag{21b}$$

Therefore, the capacity for a given ξ is

$$Q^{max}(\xi) = \frac{nz_c v_f}{1+\alpha v_f\xi} \geqslant nz_c v_f \frac{\tau z_j v_f}{1+\tau z_j v_f}.$$

Without lane changing, the capacity is $nz_c v_f$. Thus the capacity reduction caused by lane-changing traffic is up to:

$$CR \equiv \frac{nz_c v_f - Q^{max}(\xi)}{nz_c v_f} \leqslant \frac{1}{1+\tau z_j v_f} = \frac{z_c}{z_j}.$$

The exact capacity reduction is related to lane-changing parameter α, but the upperbound of capacity reduction is not.

- When $1/z_j - \alpha\tau\xi v_f^2 < 0$, $\widetilde{Q}_2(v,\xi)$ reaches its maximum at

$$z_c(\xi) = K_2(v_c(\xi),\xi), \tag{22a}$$

$$v_c(\xi) = \frac{1}{\sqrt{\alpha\tau z_j \xi}}, \tag{22b}$$

and

$$Q^{max}(\xi) = \frac{n}{\tau\left(1+\sqrt{\frac{\alpha\xi}{\tau z_j}}\right)^2} < nz_c v_f\left(1-\frac{z_c}{z_j}\right)$$

In this case, $Q(k,\xi)$ is still unimodal in k, and the capacity reduction caused by lane-changing traffic is given by:

$$CR \equiv \frac{nz_c v_f - Q^{max}}{nz_c v_f} > \frac{z_c}{z_j}.$$

4.3. Calibration and validation

In this subsection, we calibrate the lane-changing fundamental diagram with vehicle trajectory data collected in a lane-changing area on Interstate 80 in Emeryville (San Francisco), California, as shown in Fig. 3. In the road section, the mainline freeway has six lanes, including a car-pool lane (lane 1), an on-ramp from Powell Street (lane 7), and an off-ramp to Ashby Ave (lane 8). In our study we consider the car-pool lane as a regular lane, and set $n = 6$ in the lane-changing area. In FHWA's NGSIM project, vehicle trajectories were transcribed from video images collected by seven cameras, numbered 1–7 from south to north (Federal Highway Administration, 2006). Four data sets are available: Data set 1 provides vehicles' longitudinal and lateral locations every one-fifteenth of a second on December 3, 2003 between 2:35 pm and 3:05 pm; Data sets 2–4 provide locations of each vehicle every one-tenth of a second on April 13, 2005 between 4–4:15 pm, 5–5:15 pm, and 5:15–5:30 pm, respectively. Vehicle trajectories on the on-ramp and the off-ramp are also available. These data sets cover both free flow and congested traffic conditions: the congestion level increases from data sets 1 to 4.

From calibrated results of car-following behaviors in Chiabaut et al. (2010) and Yang et al. (2011), we set $\tau = 1.6$ s, and $z_j = 224$ vpmpl. In addition, we set $v_f = 60$ mph and $L = 300$ m. In Table 1, we list the average on-ramp flow-rates, ϕ, and lane-changing times, π, for four data sets. Here ϕ is calculated as the ratio of the number of on-ramp vehicles to the time duration for these vehicles entering the freeway (switching from lane 7 to lane 6). The average lane-changing durations are calculated from all lane changes in a data set: we assume that the lateral traveling distance during a lane-changing process equals 1.5 times the width of a vehicle (Refer to Fig. 10 of Jin (2010a) for an illustration of the definition). We assume that ϕ and π are both constant in the lane-changing area: $\phi = 800$ vph, and $\pi = 10$ s. Hence $\alpha = \frac{n-1}{2L}\pi = (12\ \text{m/s})^{-1} = (26.8\ \text{mph})^{-1}$, and $\alpha\phi = 30$ vpm, which also equals the average value of $\alpha\phi$ for four data sets in the table.

We simply assume that the weaving flow-rate is known and constant for the study area. Then from (18) we obtain the following fundamental diagram:

$$\epsilon = \frac{30}{k}, \tag{23a}$$

$$v = \min\left\{60, 2250\left(\frac{6}{k+30} - \frac{1}{224}\right)\right\}, \tag{23b}$$

$$q = \min\left\{60k, 2250\left(\frac{6k}{k+30} - \frac{k}{224}\right)\right\}, \tag{23c}$$

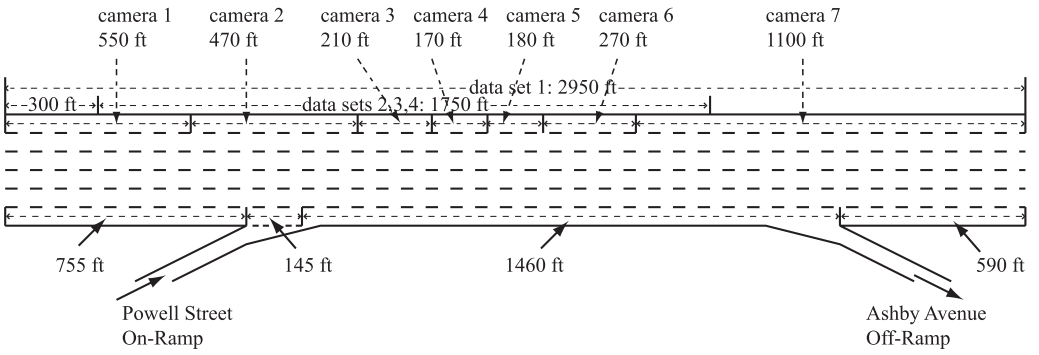

Fig. 3. A lane-changing area on I-80.

Table 1
Average on-ramp flow-rates and lane-changing times for four data sets.

Data set	On-ramp flow	Time (s)	ϕ (vph)	π (s)	$\alpha\phi$ (vpm)
1	314	1742	649	11.0	26.4
2	190	882	775	8.5	24.4
3	206	864	858	9.8	31.1
4	215	907	853	12.4	39.2

where $0 \leqslant k \leqslant 1314$ vpm. In this case, $z_c = 32.1$ vmppl, and (19) is violated. Thus q reaches the capacity at $k = \sqrt{nz_j\alpha\phi} - \alpha\phi = 170.8$ vpm, and $Q^{max}(\phi) = \frac{1}{\tau z_j}\left(\sqrt{nz_j} - \sqrt{\alpha\phi}\right)^2 = 9767.4$ vph. Without considering lane changes, the capacity is $nz_{c-}v_f = 11564.1$ vph. Therefore the capacity reduction caused by the lane-changing traffic, which is induced by the on-ramp vehicles, is $CR = 15.5\%$.

In Fig. 4, we demonstrate the observed and derived intensity-, speed-, and flow-density relations for the I-80 lane-changing area. In these figures, the circles are observed data in a road section downstream to the on-ramp in Fig. 3 between $x_a = 950$ ft and $x_b = 1850$ ft. Each point corresponds to a time interval $[t_i, t_i + T]$, where t_i is the smallest time for the first vehicle in a data set, and $T = 39, 63, 86, 100$ for four data sets respectively. Refer to (Jin, 2010b) on computations of k, v, q, and ϵ in an Edie's domain of $[x_a, x_b] \times [t_i, t_i + T]$. The solid lines correspond to the derived relations in (23), and the dashed lines correspond to relations without considering lane changes.

From Fig. 4, we can see that the derived fundamental diagram of lane-changing traffic approximately matches the observed data. However, the observed data are highly scattered, and there exist significant discrepancies between the derived curves and the observed data. Several simplifying assumptions contribute to the discrepancies and are discussed in the following. First, when deriving the lane-changing fundamental diagram, we assume steady traffic, but in reality traffic is most likely in non-steady states, as can be seen from the scatteredness in observed data. Second, the fundamental diagram in (23) is not calibrated from observations through curve fitting techniques, which was used to calibrate the relationship between ϵ and k with R-squares above 0.8 in Jin (2010a); instead, it is derived from basic car-following parameters (v_f, τ, and z_j), lane-changing parameters (L, π, and ϕ), and the number of lanes (n). Third, the flow-rate of on-ramp vehicles ϕ is assumed to be constant, but in reality it varies from 649 vph in data set 1–858 vph in data set 3. Fourth, vehicles have heterogeneous car-following and lane-changing characteristics, but in reality different vehicles can have significantly different lane-changing durations (Toledo and Zohar, 2007). Finally, impacts of lane changes caused by off-ramp vehicles are ignored in (23), but, especially in free-flow traffic, many vehicles tend to change their routes in the weaving area. Therefore, the lane-changing fundamental diagram in (23) is only a reasonable first-order approximation and can be improved in many ways.

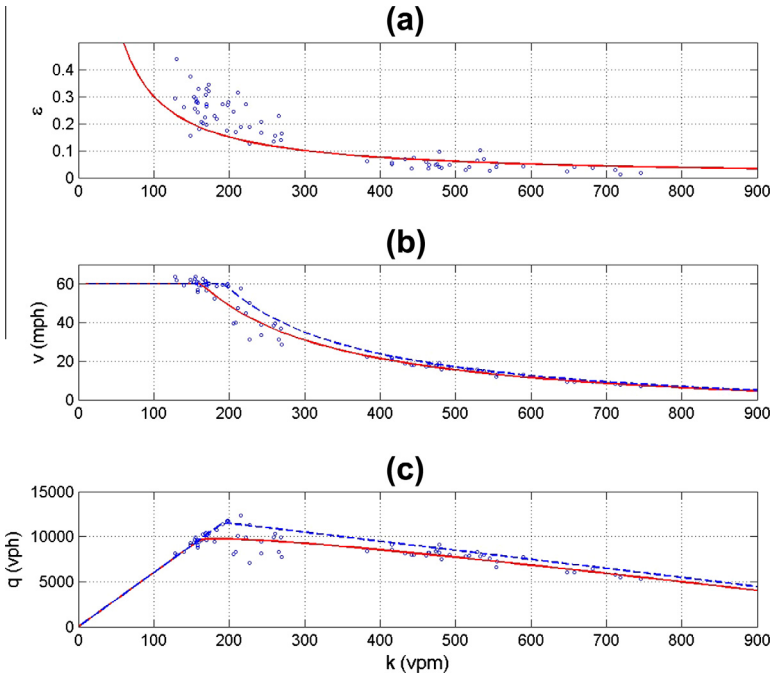

Fig. 4. Observed and derived intensity-(a), speed-(b), and flow-density (c) relations for the I-80 lane-changing area.

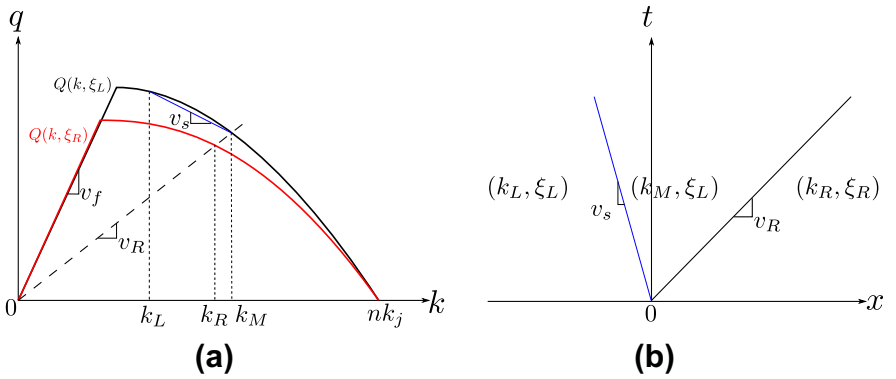

Fig. 5. A shock wave solution: (a) in the fundamental diagrams; (b) in $x-t$ space.

5. The Riemann problem

In this section, we consider the following Riemann problem for the kinematic wave model (5) in a homogeneous lane-changing area with the following initial condition[9]:

$$(k,\rho)=\begin{cases}(k_L,\rho_L), & x<0\\ (k_R,\rho_R), & x>0\end{cases}$$

which can be re-written as ($\xi_L=\rho_L/k_L$ and $\xi_R=\rho_R/k_R$):

$$(k,\xi)=\begin{cases}(k_L,\xi_L), & x<0\\ (k_R,\xi_R), & x>0\end{cases}$$

Since weaving proportions are given, we use the fundamental diagram in (20). The upstream and downstream speeds are respectively given by

$$v_L=\min\{v_f,K_2^{-1}(k_L,\xi_L)\},$$
$$v_R=\min\{v_f,K_2^{-1}(k_R,\xi_R)\}.$$

Here we assume that the fundamental diagrams of car-following traffic are the same for both upstream and downstream sections. Then the fundamental diagram of lane-changing traffic at a location is determined by the weaving proportion.

5.1. Riemann solutions

In order to solve the Riemann problem, we apply the following rules as entropy conditions (R5'): (i) Downstream vehicles always travel at the constant speed of v_R, and the weaving proportion ξ_R remains constant in the region of downstream vehicles, since downstream traffic dynamics are not affected by upstream traffic; i.e., $(k,\xi)=(k_R,\xi_R)$ in the region of $x>v_Rt$; (ii) However, the upstream vehicles have to follow the car-following rule: if $v_L<v_R$, upstream vehicles will accelerate to v_R, and a rarefaction wave initiates at $x=0$; if $v_L>v_R$, upstream vehicles will decelerate to v_R, and a shock wave initiates at $x=0$; (iii) In the region occupied by the upstream vehicles, $x<v_Rt$, the weaving proportion $\xi=\xi_L$; i.e., vehicles follow the FIFO rule such that two traffic streams do not mix up with each other. These entropy conditions can be considered as an extension to that in Ansorge (1990), which is consistent with Lax's entropy condition for the traditional LWR model.

With the aforementioned entropy conditions, the Riemann problem is equivalent to a lead-vehicle problem for the upstream vehicles (Del Castillo et al., 1994; Daganzo, 2006), since the upstream vehicles are effectively led by a vehicle traveling at v_R. A shock wave solution is shown in Fig. 5, where solutions in the $k-q$ space are shown in Fig. 5(a), and wave solutions in the $x-t$ space are shown in Fig. 5(b): the downstream traffic of k_R, ξ_R will move at a constant speed v_R; in the intermediate region vehicles from the upstream section will travel in the speed of v_R with a weaving proportion ξ_L, and the intermediate density is given by

$$k_M=K_2(v_R,\xi_L), \tag{24}$$

since $v_R\leqslant v_f$; a shock wave initiates at $x=0$ with a speed of

$$v_s=\frac{k_Lv_L-k_Mv_R}{k_L-k_M},$$

[9] Since kinematic wave propagate in a finite speed, we can effectively consider the lane-changing area to be infinitely long.

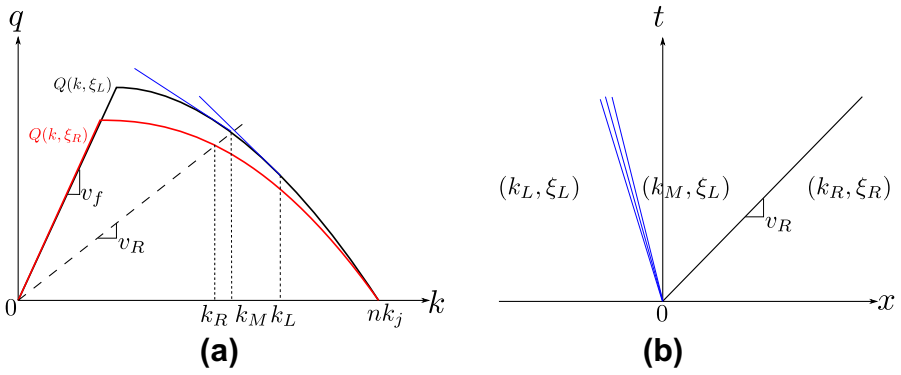

Fig. 6. A rarefaction wave solution: (a) in the fundamental diagrams; (b) in $x-t$ space.

since $k_M > k_L$. A rarefaction wave solution is shown in Fig. 6: here everything is the same except that a rarefaction wave initiates at $x = 0$, since $k_M < k_L$. In both cases, kinematic waves arising from $x = 0$ are also solutions to the Riemann problem for the traditional LWR model:

$$\frac{\partial k}{\partial t}+\frac{\partial kV(k,\xi_L)}{\partial x}=0,$$

with initial densities:

$$k=\begin{cases}k_L, & x<0\\ k_M, & x>0\end{cases}$$

5.2. Boundary fluxes in demand and supply

We define the upstream demand $D(k_L, \xi_L)$ by

$$D(k_L,\xi_L)=Q(\min\{k_L,k_c(\xi_L)\},\xi_L), \tag{25}$$

and the downstream supply $S(k_M, \xi_L)$ by

$$S(k_M,\xi_L)=Q(\max\{k_M,k_c(\xi_L)\},\xi_L), \tag{26}$$

where $k_c(\xi_L)$ is defined in (21a) and (22a). From (24), we can define the downstream supply in v_R

$$\widetilde{S}(v_R,\xi_L)=Q(\max\{K_2(v_R,\xi_L),k_c(\xi_L)\},\xi_L)=\widetilde{Q}_2(\min\{v_R,v_c(\xi_L)\},\xi_L), \tag{27}$$

where $v_c(\xi_L)$ is defined in (21b) and (22b).

From the Riemann solutions, one can verify that the boundary fluxes are given by

$$q(x=0,t)=\min\{D(k_L,\xi_L),S(k_M,\xi_L)\}=\min\{D(k_L,\xi_L),\widetilde{S}(v_R,\xi_L)\},$$
$$\phi(x=0)=\xi_L q(x=0,t).$$

These boundary fluxes are of Godunov type, since they are obtained from Riemann solutions (Godunov, 1959). We can show that the boundary fluxes satisfy the following optimization problem:

$$\max q(x=0,t), \tag{28}$$

s.t.

$$q(x=0,t)\leqslant d_L=D(k_L,\xi_L), \tag{29a}$$
$$q(x=0,t)\leqslant s_R=\widetilde{S}(V(k_R,\xi_R),\xi(x=0,t)), \tag{29b}$$

where

$$\xi(x=0,t)=\frac{\phi(x=0,t)}{q(x=0,t)}. \tag{29c}$$

In the lane-changing area, since traffic follows the FIFO principle; i.e., since traffic is in the 1-pipe regime in the sense of Daganzo (1997) and Daganzo (2002), we have $\phi(x = 0, t) = q(x = 0, t)\xi_L$, which leads to $\xi(x = 0, t) = \xi_L$. However, if upstream traffic is in the 2-pipe regime, for example, at a merging junction, then an additional relation between $\phi(x = 0, t)$ and

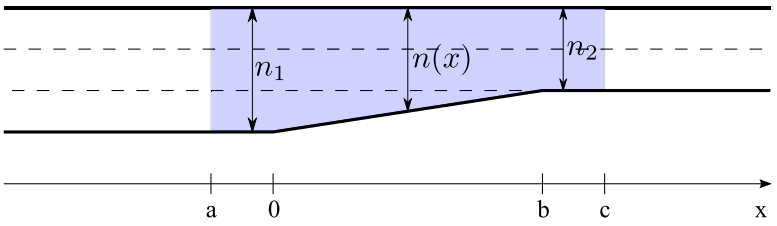

Fig. 7. The lane-changing area around a lane-drop bottleneck.

$q(x = 0, t)$ has to be introduced. The boundary flux in demand and supply can be extended for inhomogeneous lane-changing areas and readily incorporated into the Cell Transmission Model (Daganzo, 1995; Lebacque, 1996).

6. The multi-commodity LWR model for the lane-changing area around a lane-drop

In this section, we derive a multi-commodity LWR model for traffic dynamics inside the lane-changing area around a lane-drop bottleneck, as shown in Fig. 7, where n_1 lanes merge into n_2 lanes. It is reasonable to assume that vehicles on the right $n_1 - n_2$ lanes in the upstream area are weaving vehicles. Therefore, the weaving proportion inside the lane-changing area is constant: $\xi = \frac{\rho}{k} = \frac{n_1 - n_2}{n_1}$. However, the road is inhomogeneous, and the multi-commodity LWR model, (5), can be modified as

$$\frac{\partial k}{\partial t} + \frac{\partial Q(n(x), k, \xi)}{\partial x} = 0, \tag{30}$$

where $n(x)$ is the number of lanes at x.

6.1. The fundamental diagram and the Godunov fluxes

Inside the lane-changing area, we have $\alpha(x) = \frac{n(x)-1}{2}\frac{\pi}{L}$. From (20), we can obtain the location-dependent fundamental diagram

$$k = K_2(n(x), v, \xi) \equiv \frac{n(x)}{(1 + \alpha(x)\xi v)(1/z_j + \tau v)}, \tag{31a}$$

$$v = V(n(x), k, \xi) = \min\left\{v_f, K_2^{-1}(n(x), k, \xi)\right\}, \tag{31b}$$

$$q = Q(n(x), k, \xi) = \begin{cases} Q_1(n(x), k, \xi) \equiv v_f k, & k \leqslant n(x) z_c/(1 + \alpha(x)\xi v_f) \\ Q_2(n(x), k, \xi) \equiv k K_2^{-1}(n(x), k, \xi), & k > n(x) z_c/(1 + \alpha(x)\xi v_f) \end{cases} \tag{31c}$$

When $k > n(x)z_c/(1 + \alpha(x)\xi v_f)$; i.e., when $v < v_f$, q is also a function of v; i.e.,

$$q = Q_2(n(x), k, \xi) \equiv \tilde{Q}_2(n(x), v, \xi) = v K_2(n(x), v, \xi), \quad \text{when } v < v_f.$$

In addition, the lane-changing intensity is also location-dependent

$$\epsilon = E(n(x), k, \xi) = \alpha(x)\xi v = \alpha(x)\xi \min\left\{v_f, K_2^{-1}(n(x), k, \xi)\right\}.$$

In this sense, the LWR model of lane-changing traffic around a lane-drop area, (30), can be considered as a generalization of the model considered in Jin (2010a).

From the fundamental diagram, the critical density, speed, and capacity can be computed in the following two cases:

1. When $1/z_j - \alpha(x)\tau\xi v_f^2 \geqslant 0$, the total critical density $k_c(n(x), \xi) = \frac{n(x)z_c}{1+\alpha(x)\xi v_f}$, critical speed $v_c(n(x),\xi) = v_f$, and the capacity is given by

$$Q^{max}(n(x), \xi) = \frac{n(x) z_c v_f}{1 + \alpha(x) v_f \xi}. \tag{32}$$

2. When $1/z_j - \alpha(x)\tau\xi v_f^2 < 0$, the total critical density $k_c(n(x),\xi) = K_2(n(x),v_c(\xi),\xi)$, critical speed $v_c(n(x), \xi) = \frac{1}{\sqrt{\alpha(x)\tau z_j \xi}}$, and the capacity is given by

$$Q^{max}(n(x), \xi) = \frac{n(x)}{\tau\left(1 + \sqrt{\frac{\alpha(x)\xi}{\tau z_j}}\right)^2}. \tag{33}$$

Table 2
Capacities of a lane-drop area for different numbers of lanes (unit: vph).

n_1	2	3	4	5	6	7	8	9	10
$(n_1-1)z_c v_f$	1926	3852	5778	7704	9630	11,556	13,482	15,408	17,334
$Q^{max}(n_1)$	1926	3352	4738	6126	7515	8903	10,291	11,679	13,067
CR (%)	0	13	18	20	22	23	24	24	25
$Q^{max}(n_1)-Q^{max}(n_1-1)$		1426	1386	1388	1389	1388	1388	1388	1388

For the Riemann problem with upstream and downstream initial conditions (n_L, k_L, ξ) and (n_R, k_R, ξ), respectively, we can calculate the upstream demand from

$$D(n_L, k_L, \xi) = Q(n_L, \min\{k_L, z_c(n_L, \xi)\}, \xi), \tag{34}$$

and the downstream supply from

$$\widetilde{S}(n_R, k_R, \xi) = \widetilde{Q}_2(n_R, \min\{V(n_R, k_R, \xi), v_c(n_R, \xi)\}, \xi). \tag{35}$$

The boundary fluxes are given by

$$q(x=0,t) = \min\{D(n_L, k_L, \xi), \widetilde{S}(n_R, k_R, \xi)\}, \tag{36a}$$
$$\phi(x=0) = \xi q(x=0,t), \tag{36b}$$

which can be incorporated into CTM for simulations. In addition, it can be shown that the multi-commodity LWR model, (30), is well-defined with (36) as an entropy condition.

6.2. Capacities of lane-drop areas and smoothing effects of HOV lanes

In this subsection, we assume that $n_2 = n_1 - 1$, and the downstream of the lane-drop area is not congested; i.e., the lane-drop area is an active bottleneck in the sense of Daganzo (1999). In addition, we use the following car-following and lane-changing parameters from Section 4.3: $\tau = 1.6$ s, $z_j = 224$ vpmpl, $v_f = 60$ mph, $L = 300$ m, and $\pi = 10$ s. Then $z_c = 32.1$ vpmpl, and $\alpha(x) = \frac{n(x)-1}{134}$ $(\text{mph})^{-1}$. It can be shown that the capacity of the road section is determined by the downstream section when $n(x) = n_1 - 1$. Thus we have the following capacities of the lane-drop area:

1. When $(n_1-2)/n_1 \leqslant 0.3739$; i.e., when $n_1 \leqslant 3$, the capacity is
$$Q^{max}(n_1) = 1926\frac{n_1-1}{1+\frac{60}{134}\frac{n_1-2}{n_1}}.$$
2. When $(n_1-2)/n_1 > 0.3739$; i.e., when $n_1 \geqslant 4$, the capacity is
$$Q^{max}(n_1) = 2250\frac{n_1-1}{\left(1+\frac{1}{3.6525}\sqrt{\frac{n_1-2}{n_1}}\right)^2}$$

For different numbers of lanes, n_1, the capacities are listed in Table 2. In particular, when $n_1 = 2$; i.e., when two lanes drop into one lane, $Q^{max}(2) = 1926$ vph, which is the single-lane capacity without lane changes. Without lane-changing effects, the capacity is $(n_1-1)z_c v_f$. From the table we can see that lane changes inside a lane-drop area can significantly reduce the capacity, and the capacity reduction ratio increases with the number of lanes, since more lanes would induce more disruptive lane changes. The table also shows the differences, $Q^{max}(n_1) - Q^{max}(n_1-1)$, which are around 1400 vph.

In Chen et al. (2005), Menendez and Daganzo (2007), Daganzo and Cassidy (2008), Cassidy et al. (2009) and Cassidy et al. (2010), the smoothing effect of HOV lanes has been observed around various bottlenecks: when carpool lanes or other lane restrictions are implemented, higher discharging rates on regular lanes can be achieved. In particular, in Cassidy et al. (2010), it was shown that the activation of a carpool lane can increase the throughput on regular lanes by 300–600 vph for a four-lane freeway. In Appendix A of Cassidy et al. (2010), it was argued that the activation of the carpool lane discourages lane changes inside a bottleneck and, therefore, increases throughput.

Here we attempt to explain such smoothing effects of HOV lanes in a lane-drop area with the proposed lane-changing fundamental diagram, (31), by considering the left-most lane as an HOV lane. For the purpose of simplicity, we assume that all HOV's are always on the HOV lane, and thus only low-occupancy vehicles need to switch lanes in the lane-drop area. If the total number of upstream lanes is n_1, after implementing an HOV lane, the lane-drop area is equivalent to one with $n_1 - 1$ lanes. If we denote the throughput of the HOV lane by Q_{HOV}, then the total capacity of the lane-drop area after implementing an HOV lane becomes

$$\widetilde{Q}^{max}(n_1) = Q_{HOV} + Q^{max}(n_1 - 1).$$

We know that, before implementing an HOV lane, the capacity of the lane-drop area is $Q^{max}(n_1)$. Thus the smoothing effect of an HOV lane is defined as the difference in the capacities after and before implementing an HOV lane:

$$\widetilde{Q}^{max}(n_1) - Q^{max}(n_1) = Q_{HOV} + Q^{max}(n_1 - 1) - Q^{max}(n_1) \approx Q_{HOV} - 1400.$$

Therefore, the total capacity can be increased by implementing an HOV lane if the HOV lane is well utilized; i.e., if its throughput is greater than 1400 vph. In particular, if its throughput equals the lane capacity, 1926, then the total throughput can be increased by around 500 vph, which is consistent with the aforementioned observations.[10] This confirms that lane changes are the primary reason of HOV lanes' smoothing effects (Cassidy et al., 2010). The consistency also demonstrates that the multi-commodity LWR theory of lane-changing traffic flow can be used to quantify such effects analytically, as long as car-following and lane-changing parameters are well calibrated.

7. Conclusion

In this study, a multi-commodity LWR model was proposed for lane-changing traffic flow, in which weaving and non-weaving vehicles belong to different commodities. The new model is a behavioral counterpart of the phenomenological model proposed in Jin (2010a,b). Based on a macroscopic behavioral model of lane-changing traffic flow, a fundamental diagram was derived for lane-changing traffic with parameters determined by car-following and lane-changing characteristics as well as road geometry and traffic composition. In particular, fundamental diagrams based on a triangular car-following fundamental diagram were calibrated and validated with NGSIM data. Inside a homogeneous lane-changing area, the Riemann problem for the LWR model was solved, and the corresponding demand and supply functions were defined. Finally the model was applied to study lane-changing traffic dynamics and capacities inside a lane-drop area, and the smoothing effect of HOV lanes was quantified and shown to be consistent with observations in existing studies. Both theoretical and empirical studies demonstrate that systematic lane changes can significantly reduce traffic capacities.

We made two key assumptions when deriving a multi-commodity fundamental diagram of lane-changing traffic flow: the number of lane changes is proportional to the weaving flow-rate, and the durations are the same for all lane changes. From the validation studies, we can see that these assumptions can be considered as first-order approximations to macroscopic lane-changing behaviors. It is possible to develop higher-order approximations, but the resulted model could lose its mathematical tractability. In the future, we will be interested in studying lane-changing traffic dynamics around a merging junction, where the weaving flow-rate is determined by the merging process. For this purpose, there is a need to develop an integrated merging and lane-changing traffic flow model. Traffic dynamics inside other lane-changing areas could also be studied with the multi-commodity LWR model.

In this study we showed that systematic lane changes can reduce the capacity of a road section, and the reduction ratio is highly related to the proportion of weaving vehicles. Therefore, a sudden increase in weaving proportions could cause capacity drop (Hall and Agyemang-Duah, 1991; Banks, 1991; Cassidy and Rudjanakanoknad, 2005; Chung et al., 2007). However, in an area with capacity drop, the flow-density relation is believed to be of the reverse-lambda shape (Koshi et al., 1983). Since the fundamental diagrams in this study are still continuous, the lane-changing model may not be able to fully explain the occurrence of capacity drops. In the future, we will be interested in investigating the impacts of lane changes on capacity drops and other traffic phenomena.

In a fundamental diagram of lane-changing traffic flow, the capacity decreases in the lane-changing intensity, which increases in the lane-changing duration, the number of lanes, and the weaving proportion but decreases in the length of the lane-changing area. In addition to HOV lane management strategies, it is possible to alleviate the bottleneck effect of lane-changing traffic by prolonging the lane-changing area and reducing the lane-changing maneuvering time through advanced traffic management strategies. The model developed in this study can guide the development and evaluation of such strategies.

Acknowledgement

This work was partially funded by the University of California Transportation Center. Comments by Qijian Gan, Anupam Srivastava, and two anonymous reviewers are appreciated.

References

Ahn, S., Cassidy, M., 2007. Freeway traffic oscillations and vehicle lane-change maneuvers. In: Proceedings of the 17th International Symposium on Traffic and Transportation Theory, pp. 691–710.

Ansorge, R., 1990. What does the entropy condition mean in traffic flow theory? Transportation Research Part B 24 (2), 133–143.

Banks, J.H., 1991. The two-capacity phenomenon: some theoretical issues. Transportation Research Record: Journal of the Transportation Research Board 1320, 234–241.

Benzoni-Gavage, S., Colombo, R., 2003. An *n*-populations model for traffic flow. European Journal of Applied Mathematics 14 (05), 587–612.

[10] Even though the bottleneck studied in Cassidy et al. (2010) is downstream to a merging junction, it is similar to a lane-drop bottleneck for congested traffic.

Bürger, R., García, A., Karlsen, K., Towers, J., 2008. A family of numerical schemes for kinematic flows with discontinuous flux. Journal of Engineering Mathematics 60 (3), 387–425.
Burger, R., Kozakevicius, A., 2007. Adaptive multiresolution weno schemes for multi-species kinematic flow models. Journal of Computational Physics 224 (2), 1190–1222.
Cassidy, M., Daganzo, C.F., Jang, K., Chung, K., 2009. Spatiotemporal effects of segregating different vehicle classes on separate lanes. In: Proceedings of the 18th International Symposium on Transportation and Traffic Theory, pp. 57–74.
Cassidy, M., Jang, K., Daganzo, C.F., 2010. The smoothing effect of carpool lanes on freeway bottlenecks. Transportation Research Part A 44 (2), 65–75.
Cassidy, M., Rudjanakanoknad, J., 2005. Increasing the capacity of an isolated merge by metering its on-ramp. Transportation Research Part B 39 (10), 896–913.
Cassidy, M., Skabardonis, A., May, A.D., 1989. Operation of major freeway weaving sections: recent empirical evidence. Transportation Research Record: Journal of the Transportation Research Board 1225, 61–72.
Chanut, S., Buisson, C., 2003. Macroscopic model and its numerical solution for two-flow mixed traffic with different speeds and lengths. Transportation Research Record: Journal of the Transportation Research Board 1852, 209–219.
Chen, C., Varaiya, P., Kwon, J., 2005. An empirical assessment of traffic operations. In: Proceedings of the 16th International Symposium on Transportation and Traffic Theory, pp. 19–21.
Chiabaut, N., Leclercq, L., Buisson, C., 2010. From heterogeneous drivers to macroscopic patterns in congestion. Transportation Research Part B 44 (2), 299–308.
Chung, K., Rudjanakanoknad, J., Cassidy, M., 2007. Relation between traffic density and capacity drop at three freeway bottlenecks. Transportation Research Part B 41 (1), 82–95.
Daganzo, C.F., 1995. The cell transmission model II: network traffic. Transportation Research Part B 29 (2), 79–93.
Daganzo, C.F., 1997. A continuum theory of traffic dynamics for freeways with special lanes. Transportation Research Part B 31 (2), 83–102.
Daganzo, C.F., 1999. Remarks on traffic flow modeling and its applications. In: Brilon, W., Huber, F., Schreckenberg, M., Wallentowitz, H. (Eds.), Proceedings of Traffic and Mobility: Simulation, Economics and Environment. Springer Verlag, pp. 105–115.
Daganzo, C.F., 2002. A behavioral theory of multi-lane traffic flow. Part I: Long homogeneous freeway sections. II: Merges and the onset of congestion. Transportation Research Part B 36 (2), 131–169.
Daganzo, C.F., 2006. In traffic flow, cellular automata = kinematic waves. Transportation Research Part B 40 (5), 396–403.
Daganzo, C.F., Cassidy, M., 2008. Effects of high occupancy vehicle lanes on freeway congestion. Transportation Research Part B 42 (10), 861–872.
Daganzo, C.F., Lin, W.-H., Del Castillo, J.M., 1997. A simple physical principle for the simulation of freeways with special lanes and priority vehicles. Transportation Research Part B 31 (2), 103–125.
Del Castillo, J., Pintado, P., Benitez, F., 1994. The reaction time of drivers and the stability of traffic flow. Transportation Research Part B 28 (1), 35–60.
Del Castillo, J.M., Benitez, F.G., 1995a. On the functional form of the speed-density relationship – I: General theory. Transportation Research Part B 29 (5), 373–389.
Del Castillo, J.M., Benitez, F.G., 1995b. On the functional form of the speed-density relationship – II: Empirical investigation. Transportation Research Part B 29 (5), 391–406.
Eads, B.S., Rouphail, N.M., May, A.M., Hall, F., 2000. Freeway facility methodology in "Highway Capacity Manual" 2000. Transportation Research Record: Journal of the Transportation Research Board 1710, 171–180.
Edie, L., 1963. Discussion on traffic stream measurements and definitions. In: Proceedings of the Second International Symposium on the Theory of Road Traffic Flow, pp. 139–154.
Federal Highway Administration, 2006. Next Generation SIMulation Fact Sheet. Tech. rep., FHWA-HRT-06-135.
Gipps, P.G., 1986. A model for the structure of lane changing decisions. Transportation Research Part B 20 (5), 403–414.
Godunov, S.K., 1959. A difference method for numerical calculations of discontinuous solutions of the equations of hydrodynamics. Matematicheskii Sbornik 47 (3), 271–306, in Russia.
Golob, T.F., Recker, W.W., Alvarez, V.M., 2004. Safety aspects of freeway weaving sections. Transportation Research Part A 38 (1), 35–51.
Greenshields, B.D., 1935. A study in highway capacity. Highway Research Board Proceedings 14, 448–477.
Haberman, R., 1977. Mathematical Models. Prentice Hall, Englewood Cliffs, NJ.
Hall, F.L., Agyemang-Duah, K., 1991. Freeway capacity drop and the definition of capacity. Transportation Research Record: Journal of the Transportation Research Board 1320, 91–98.
Hidas, P., 2002. Modelling lane changing and merging in microscopic traffic simulation. Transportation Research Part C 10 (5–6), 351–371.
Isaacson, E.I., Temple, J.B., 1992. Nonlinear resonance in systems of conservation laws. SIAM Journal on Applied Mathematics 52 (5), 1260–1278.
Jin, W.-L., 2010a. A kinematic wave theory of lane-changing traffic flow. Transportation Research Part B 44 (8–9), 1001–1021.
Jin, W.-L., 2010b. Macroscopic characteristics of lane-changing traffic. Transportation Research Record: Journal of the Transportation Research Board 2188, 55–63.
Jin, W.-L., 2012. A kinematic wave theory of multi-commodity network traffic flow. Transportation Research Part B 46 (8), 1000–1022.
Jin, W.-L., Zhang, H.M., 2004. A multicommodity kinematic wave simulation model of network traffic flow. Transportation Research Record: Journal of the Transportation Research Board 1883, 59–67.
Kesting, A., Treiber, M., Helbing, D., 2007. General lane-changing model MOBIL for car-following models. Transportation Research Record: Journal of the Transportation Research Board 1999, 86–94.
Koshi, M., Iwasaki, M., Ohkura, I., 1983. Some findings and an overview on vehicular flow characteristics. In: Proceedings of the Eighth International Symposium on Transportation and Traffic Theory, pp. 403–426.
Laval, J., Cassidy, M., Daganzo, C.F., 2005. Impacts of lane changes at merge bottlenecks: a theory and strategies to maximize capacity. In: Proceedings of the Traffic and Granular Flow Conference.
Laval, J., Daganzo, C.F., 2006. Lane-changing in traffic streams. Transportation Research Part B 40 (3), 251–264.
Laval, J., Leclercq, L., 2008. Microscopic modeling of the relaxation phenomenon using a macroscopic lane-changing model. Transportation Research Part B 42 (6), 511–522.
Lax, P.D., 1972. Hyperbolic Systems of Conservation Laws and The Mathematical Theory of Shock Waves. SIAM, Philadelphia, PA.
Lebacque, J.P., 1996. The Godunov scheme and what it means for first order traffic flow models. In: Proceedings of the 13th International Symposium on Transportation and Traffic Theory, pp. 647–678.
Leisch, J.E., 1979. A new technique for design and analysis of weaving sections on freeways. ITE Journal 49 (3), 26–29.
Lighthill, M.J., Whitham, G.B., 1955. On kinematic waves: II. A theory of traffic flow on long crowded roads. Proceedings of the Royal Society of London A 229 (1178), 317–345.
Menendez, M., Daganzo, C.F., 2007. Effects of HOV lanes on freeway bottlenecks. Transportation Research Part B 41 (8), 809–822.
Munjal, P.K., Hsu, Y.S., Lawrence, R.L., 1971. Analysis and validation of lane-drop effects of multilane freeways. Transportation Research 5 (4), 257–266.
Newell, G., 2002. A simplified car-following theory: a lower order model. Transportation Research Part B 36 (3), 195–205.
Newell, G.F., 1993. A simplified theory of kinematic waves in highway traffic I: General theory. II: Queuing at freeway bottlenecks. III: Multi-destination flows. Transportation Research Part B 27 (4), 281–313.
Ngoduy, D., 2010. Multiclass first-order modelling of traffic networks using discontinuous flow-density relationships. Transportmetrica 6 (2), 121–141.
Patire, A.D., Cassidy, M.J., 2011. Lane changing patterns of bane and benefit: observations of an uphill expressway. Transportation Research Part B 45 (4), 656–666.

Rakha, H., Zhang, Y., 2006. Analytical procedures for estimating capacity of freeway weaving, merge, and diverge sections. Journal of Transportation Engineering 132, 618.
Richards, P.I., 1956. Shock waves on the highway. Operations Research 4 (1), 42–51.
Roess, R.P., McShane, W.R., Pignataro, L.J., 1974. Configuration, design, and analysis of weaving sections. Transportation Research Record: Journal of the Transportation Research Board 489, 1–12.
Smoller, J., 1983. Shock Waves and Reaction–Diffusion Equations. Springer-Verlag, New York.
Toledo, T., Koutsopoulos, H.N., Ben-Akiva, M.E., 2003. Modeling integrated lane-changing behavior. In: Proceedings of Transportation Research Board Annual Meeting.
Toledo, T., Zohar, D., 2007. Modeling duration of lane changes. Transportation Research Record: Journal of the Transportation Research Board 1999, 71–78.
van Lint, J.W.C., Hoogendoorn, S.P., Schreuder, M., 2008. Fastlane: new multiclass first-order traffic flow model. Transportation Research Record: Journal of the Transportation Research Board 2088, 177–187.
Wong, G.C.K., Wong, S.C., 2002. A multi-class traffic flow model: an extension of LWR model with heterogeneous drivers. Transportation Research Part A 36 (9), 827–841.
Yang, H., Gan, Q., Jin, W.-L., 2011. Calibration of a family of car-following models with retarded linear regression methods. In: Proceedings of Transportation Research Board Annual Meeting.
Yang, Q., 1997. A simulation laboratory for evaluation of dynamic traffic management systems. Ph.D. thesis, Massachusetts Institute of Technology, Cambridge, Massachusetts.
Zhang, H.M., Jin, W.-L., 2002. Kinematic wave traffic flow model for mixed traffic. Transportation Research Record: Journal of the Transportation Research Board 1802, 197–204.